Nanotechnology **18** (2007) 285701 (7pp) doi:10.1088/0957-4484/18/28/285701

Resonant Raman scattering study of CdSe nanocrystals passivated with CdS and ZnS

V M Dzhagan[1], M Ya Valakh[1], A E Raevskaya[2], A L Stroyuk[2], S Ya Kuchmiy[2] and D R T Zahn[3]

[1] Institute of Semiconductors Physics of National Academy of Sciences of Ukraine, prospekt Nauky 41, 03028 Kyiv, Ukraine
[2] Institute of Physical Chemistry, National Academy of Sciences of Ukraine, prospekt Nauky 31, 03028 Kyiv, Ukraine
[3] Institut für Physik, Technische Universität, Reichenhainer Straße 70, D-09107 Chemnitz, Germany

E-mail: dzhagan@isp.kiev.ua

Received 7 February 2007, in final form 4 May 2007
Published 15 June 2007
Online at stacks.iop.org/Nano/18/285701

Abstract
CdSe nanocrystals (NCs) were obtained from cadmium sulfate and sodium selenosulfate in aqueous gelatin solutions. A near-bandgap emission of CdSe NCs was noticeably enhanced after passivation with CdS or ZnS. Resonant Raman scattering spectra of the passivated NCs revealed new peaks attributed to the formation of the sulfide shells around CdSe cores. The peaks observed for the CdSe/CdS core–shell NCs near 280 cm^{-1} were attributed to LO vibrations within a thin CdS passivating layer. Observation of the peak in the same frequency range for CdSe/ZnS is discussed within an assumption of alloying at the core–shell interface. Notable changes in the Raman spectra at different excitation wavelengths and shell parameters were attributed to the resonant and size-selective nature of the Raman process.

1. Introduction

In semiconductor nanocrystals (NCs) and other nanosized systems with the number of surface atoms comparable to that of the inner ones, the surface plays a crucial role in determining the physical properties of the structures and affecting their applications [1]. As the surface atoms act as defect states, trapping charge carriers and deteriorating the emission properties of the NCs, a number of passivation procedures have been developed in order to diminish their negative effect [1–4]. Organic ligands cannot passivate both cationic and anionic surface traps simultaneously [2]. Particles passivated by a layer of a wider-bandgap semiconductor material (so-called 'core–shell' nanocrystals) are more robust than organic-passivated nanocrystals and therefore have greater tolerance with respect to the processing conditions necessary for incorporation into solid structures [3, 5–8]. In this case non-radiative decay channels through surface states are not accessible for electrons confined inside the core and therefore such core–shell structures show higher photoluminescence (PL) quantum yield [2, 6, 8] and other benefits related to the tuning of the bandgap in two materials.

Significant progress has already been achieved in the synthesis of CdSe NCs passivated with a single layer of sulfide or selenide using, for example, CdS [2, 9], ZnS [6, 8, 10] and ZnSe [11, 12], as well as with multilayer shells (quantum dot—quantum well structures) [13]. For a better understanding of the nature of factors governing the changes in the PL efficiency, an insight into the changes in the structure of the CdSe NC shell and of the core–shell interface is required. While the internal structure of the core in the NCs can be studied by high-resolution transmission electron microscopy (HRTEM) [8], the internal structure of the shell and the interface between core and shell are hardly discernible. X-ray diffraction (XRD) analysis shows a clear contribution from, for example, ZnS shell only for samples with high ZnS coverage because the scattering factors of ZnS are smaller than those of CdSe [8]. At the same time, the potential of resonant Raman scattering (RRS) in exploring the structure of even sub-monolayer-thick shells of semiconductor core–shell NCs has recently been demonstrated [14]. Contrary to electronic properties of the core–shell NCs which have extensively been studied by many research groups, there exist only a few studies on the vibrational properties of such systems [12, 14–16].

 © 2007 IOP Publishing Ltd Printed in the UK

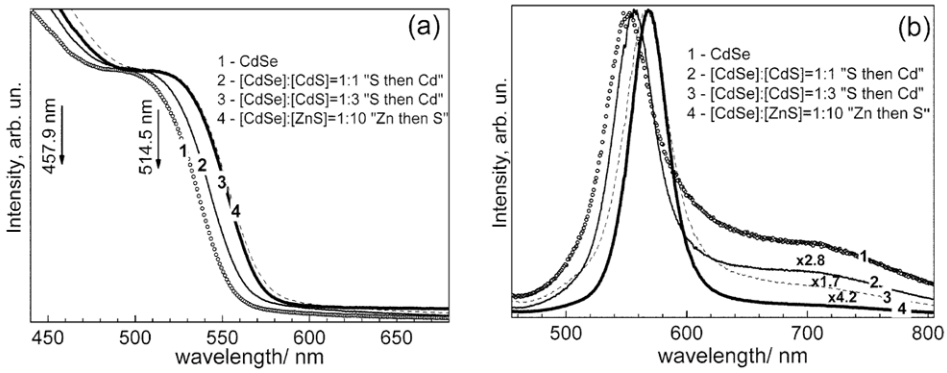

Figure 1. Normalized optical absorption (a) and PL (b) spectra of bare CdSe as well as CdSe/CdS and CdSe/ZnS core–shell NC samples. PL spectra were excited with 441.7 nm laser light. Arrows in (a) show the wavelengths used for excitation of the Raman spectra.

Table 1. Frequencies, linewidths and intensities of the Raman peaks observed for CdSe/CdS and CdSe/ZnS core–shell NC samples. Each value of the CdS-like peak intensity is defined relatively to the LO_{CdSe} peak in the same spectrum.

		CdSe-like peak			CdS-like peak		
Sample	λ_{exc} (nm)	ν_{LO} (cm^{-1}) (±0.4)[a]	Γ_{LO} (cm^{-1}) (±0.4)[a]	ν_{SO} (cm^{-1}) (±1.0)[a]	ν (cm^{-1}) (±0.8)[a]	Γ (cm^{-1}) (±0.8)[a]	I (au) (±0.2)[a]
CdSe	514.5	206.6	15.0	177.4	—	—	—
Non-passivated	457.9	206.0	15.6	180.0	—	—	—
[CdSe]:[CdS] = 1:0.5	514.5	206.0	12.1	181.7	277.0	37.4	0.2
Cd then S	457.9	203.4	15.4	186.7	282.0	54.0	0.5
[CdSe]:[CdS] = 1:1	514.5	205.7	12.5	181.6	278.3	24.0	0.3
Cd then S	457.9	203.2	13.2	185.4	283.3	55.0	1.2
[CdSe]:[CdS] = 1:1	514.5	205.8	12.2	180.4	277.8	28.3	0.2
S then Cd	457.9	203.7	13.4	189.5	278.3	48.0	1.0
[CdSe]:[CdS] = 1:3	514.5	205.5	9.6	183.7	281.0	27.4	0.4
S then Cd	457.9	202.0	12.8	187.5	283.3	49.0	1.4
[CdSe]:[ZnS] = 1:1	514.5	205.3	8.8	183.0	283.0	32.0	0.8
S then Zn	457.9	202.4	11.3	193.0	289.0	35.0	2.1

[a] The values of the experimental error are given in parentheses.

In the present paper, we discuss the results of a resonant Raman scattering study of a series of CdSe NCs synthesized in aqueous solutions from sodium selenosulfate and subsequently passivated with cadmium or zinc sulfide.

2. Experimental details

The series of samples under study consisted of CdSe NCs, both bare and passivated with CdS or ZnS. CdSe NCs were synthesized in a solution containing cadmium sulfate, gelatine and sodium selenosulfate. The details of the preparation of CdSe NCs both in solutions and in glass-anchored gelatin films, as well as their extended optical characterization, can be found elsewhere [17]. Passivation of CdSe NCs with CdS or ZnS was achieved by addition of measured volumes of $CdSO_4$ or $Zn(NO_3)_2$ solutions followed by stirring for 5–10 min and subsequent addition of an equimolar amount of sodium sulfide solution. The passivation was performed at several core-to-shell volumes and two ways of passivation: with the Cd(Zn)-supplying reagent being added before the sulfur-containing one ('Cd(Zn)—then S' scheme) and vice versa ('S—then Cd(Zn)') (table 1).

Absorption spectra of the films were recorded using a Specord M40 double-beam spectrophotometer. Raman and photoluminescence (PL) spectra were recorded using a triple monochromator Raman system (Dilor XY 800) equipped with a charge-coupled device (CCD) camera for multichannel detection. Excitation of the spectra was made with a series of Ar^+- and He–Cd laser lines. The spectral resolution of the Raman spectra and PL spectra was 2 cm^{-1} and 1 nm, respectively. All the measurements were performed at room temperature on the NCs embedded into films of the stabilizing polymer (gelatine).

3. Results and discussion

As follows from the absorption and PL measurements (figure 1), the obtained CdSe nanocrystals reveal a typical confinement-related feature at 496 nm in the absorption spectrum, corresponding to the HOMO–LUMO transition [18]. The average CdSe nanocrystal diameter d, determined from the absorption edge energy position based on dependences $E(d)$ derived in [19, 20], is about 2.6 ± 0.3 nm (curve 1).

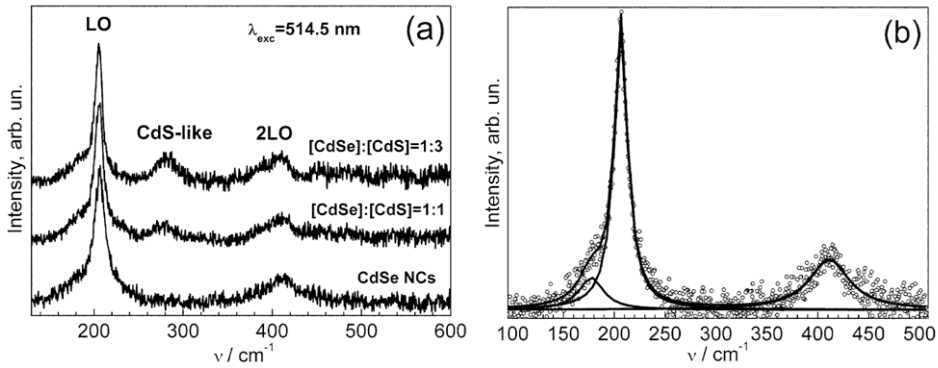

Figure 2. (a) Resonant Raman scattering spectra of CdSe and CdSe/CdS passivated NCs ('S–then Cd' scheme). (b) An example of fitting the main Raman peak of CdSe NCs with using two Lorentzians.

The PL spectrum of the initial CdSe NCs consists of a relatively sharp near-band-edge emission peak centred at 550 nm and a weak broad (FWHM $\sim$ 100 nm) band around 700 nm, significantly redshifted from the NC absorption edge and obviously caused by surface states [3, 21]. Following the procedure developed in [22], CdSe NCs size dispersion was estimated from their absorption and PL spectra to be about $15 \pm 5\%$.

As follows from figure 1, surface passivation results in a shift of the absorption and emission spectra to lower energies. This shift has been observed for different core–shell materials and explained by partial tunnelling of the electron wavefunction into the shell [2, 6, 8, 14]. The magnitude of the shift increases with the shell thickness or, in the case of equally thick shells, for the shell made of a lower bandgap material. The effect of the shell formation on the PL spectra is revealed, along with the 'red' shift, as a remarkable increase in the intensity of the near-edge emission—by a factor of up to $\sim$4—and suppression of the 'trap' emission band (figure 1). The detailed optical study of the core–shell NCs is reported elsewhere [23].

The Raman spectrum of the non-passivated CdSe NCs excited with 514.5 nm line of an Ar^+ ion laser (figure 2, curve 1) contains peaks related to the longitudinal optical (LO) phonon at 206.6 cm^{-1} and its overtone (2LO) at 411 cm^{-1}. The downward shift of the LO peak from its position for bulk CdSe at 210 cm^{-1} [24] is frequently observed for NC sizes below 10 nm due to the effect of spatial confinement of phonons in NCs [25–28]. The presence of strain has been identified in a wide range of NC samples and found to have a remarkable effect on the phonon spectra of NCs, opposing the effect of confinement [25, 26, 29, 30, 43].

The LO peaks of all the samples are observed with a low-frequency 'shoulder' which is typical for NCs of such small size and ascribed to the effect of phonon confinement [27] and/or to the contribution of the surface optical (SO) vibrations [31]. Obviously these two effects are always present in the spectra of small NCs. A satisfactory curve fitting of the spectra was achieved with using two Lorentzian profiles, representing LO and SO peaks, correspondingly (figure 2(b), table 1).

In the Raman spectra of the NCs passivated with CdS an additional peak at $\sim$280 cm^{-1} is observed as compared to bare CdSe NCs (figure 2). As the frequency of the Raman-active LO phonon in bulk CdS is 305 cm^{-1} [32] and decreases down to 280–300 cm^{-1} in thin layers and superlattices due to a combined effect of strain and phonon confinement [33], the observed peak can be attributed to the LO phonon in the CdS shell. Such a downward shift from the bulk LO phonon frequency value in the present case can also result from phonon confinement and strain. Since the shift is fairly large, one can hardly attribute it solely to confinement effects, for which a shift of less than about 5 cm^{-1} could be expected based on the experimental results for thin epitaxial CdS layers [33]. The significant broadening of the peak can be a result of phonon confinement and non-homogeneity of the very thin passivating layer.

In the case of small CdS concentration in the parental solutions (not exceeding the CdSe concentration), we did not observe any difference in the Raman spectra of the samples for two different passivation sequences ('Cd–then S' or 'S–then Cd') (table 1). This is in agreement with the shifts of absorption and near-bandgap PL maxima of these NCs [23]. The intensity of the PL was, however, found to be much more sensitive to the shell growth parameters at these small shell thicknesses [23].

The Raman spectrum of the sample with a higher thickness of CdS shell ([CdSe]:[CdS] = 1:3) differs from that with [CdSe]:[CdS] = 1:1 and the same passivation scheme 'S then Cd'. A higher frequency of the CdS-like peak for the former sample is accompanied with an increase in its intensity (figure 2). Both the absorption and PL bands of this sample show larger 'red' shifts with respect to the unpassivated CdSe NCs spectrum, as compared to the case of [CdSe]:[CdS] = 1:1, evidently indicating an increase of the thickness of the passivating layer (figure 1).

The upward shift of the CdS-like Raman peak with addition of more CdS may be partially a consequence of the shell thickness increase due to weakening of the phonon confinement in the thicker shell. The increase of this peak frequency due to changes in the strain state of the shell with increase of its thickness is less likely. Due to the 4% lattice mismatch between CdS and CdSe, the growth of the CdS shell on CdSe NC can lead to a noticeable compressive strain in the CdSe core and a tensile strain in the CdS shell. An increase of the shell thickness will lead to an increase of the compression in the core and a reduction of the tensile strain

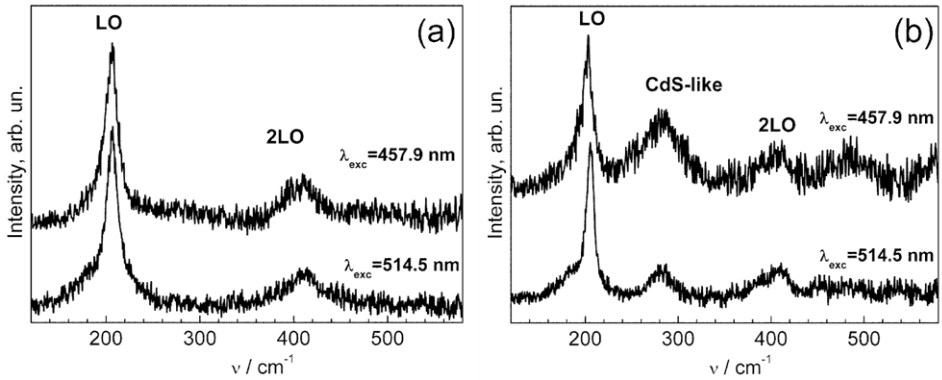

Figure 3. Resonant Raman scattering spectra excited with 514.5 and 457.9 nm laser lines for CdSe (a) and CdSe/CdS (b) NCs.

in the shell, if the strain is not relieved through the formation of dislocations. The decreased tensile strain in the shell can result in the observed frequency increase of the CdS-like peak. However, the observed shift to lower frequencies of the CdSe phonon peak does not confirm such an assumption about the strain redistribution on increasing shell thickness. The growth of the CdS-like peak intensity in the case of CdSe/CdS NCs is unlikely to be directly related to the augmentation of the scattering (shell) volume. We relate it to a decrease of the energy of the resonant electronic transition in the shell with its thickness increase, resulting in a better matching of the resonant conditions. The importance of resonant conditions for observation of this peak is discussed below in more detail. The increase of both the intensity and the width of the CdS-like peak at shorter excitation wavelength λ_{exc} (figure 3) can be the result of non-uniformity of the shell thickness among the NCs. At shorter λ_{exc} the transition energy of more shells matches the resonance conditions, leading to a increase of both the intensity and the width of the shell-related peak.

The frequency of the surface optical phonon peaks of the CdSe core ν_{SO} increases only slightly in the passivated samples (table 1), indicating that no significant compressive strain appears at the core–shell interface. Due to their surface localization, the SO phonons are supposed to be more sensitive to the strain at the interface than LO phonons inside the core. We have calculated ν_{SO} CdSe NC embedded in gelatin using the same formalism as in [14] and the same values of ν_{TO}(CdSe bulk) $= 167.5$ cm^{-1}, bulk dielectric constants of CdSe $\varepsilon_\infty = 6.1$, $\varepsilon_0 = 9.3$ and that of gelatin $\varepsilon_{GEL} = 2.37$. The calculated $\nu_{SO} = 193$ cm^{-1} shows quite a large discrepancy with the experimental value of 177–180 cm^{-1}.

In order to explain the experimentally measured values of ν_{SO} being about 10 cm^{-1} below those calculated for a spherical NC, the authors of [34] involved a significantly prolate (ellipsoidal) shape of the NC (with aspect ratio as high as 1.86 for 3.6 nm NCs). Besides, the arrangement of the atoms on the NC surface and their binding to matrix molecules are supposed to affect the ν_{SO} value as well. As both of the latter effects were found to influence the frequency of the core LO phonon [29, 35], they are expected to have even greater influence on the surface phonons. The authors of [16] observed hardening of the surface mode with the decrease of the NC size and assessed this to a stronger compression of smaller NCs by the glass matrix. Quite complex effects of the ZnS shell deposition on SO and LO phonons frequency of the core were observed in [14].

Note that, although the experimental evidence of shell-induced strain inside the core were demonstrated for a number of core–shell structures [10–12, 29], a detailed study of strain evolution in the shell and at the core–shell interface is still lacking.

Figure 4 shows resonant Raman scattering spectra of CdSe NCs passivated with ZnS. A Raman peak, observed for CdSe/ZnS NCs at almost the same frequency as that of the CdS-like phonon in CdSe/CdS NCs, was quite surprising. As far as we know, only one observation of the Raman peak related to the ZnS shell of CdSe/ZnS NCs was reported [14]. It should be noted that the position of the ZnS-shell-related phonon peak in [14] almost coincided with that of the LO phonon in bulk ZnS and did not change with the increase of the shell thickness from 0.5 to 3.4 monolayers (ML). Based only on simple considerations of phonon confinement and lattice mismatch-induced strain in a thin ZnS layer [27], one would expect this peak to be much more shifted downwards from the bulk position, with its frequency increasing with the shell thickness.

A calculation of the LO phonon frequency for thin ZnS layer grown coherently on a CdSe substrate with a mismatch strain of 11% [36] gives a value of about 300 cm^{-1}—close to that we observe for CdSe/ZnS NCs. However, in the case of growth on spherical NCs, the ZnS lattice has more freedom to relax the strain than in the two-dimensional case and, therefore, we would not relate the observed peak to a fully strained ZnS shell. Another important argument against the ZnS phonon-related origin of the observed peak is the large bandgap energy expected for a thin ZnS shell (3.7 eV for bulk), which precludes the resonant Raman scattering from the shell. Resonant excitation is, however, a necessary condition to register the Raman signal from the extremely small scattering volumes like NCs dispersed in a matrix.

The presence of a CdS-like peak and the absence of a ZnS phonon peak in the spectra of CdSe/ZnS NCs under investigation, as opposite to [14], seem quite unexpected. It is reasonable to assume that, due to the difference in growth conditions, the core–shell structure in our case is different from that reported in [14]. In particular, a very small ZnS

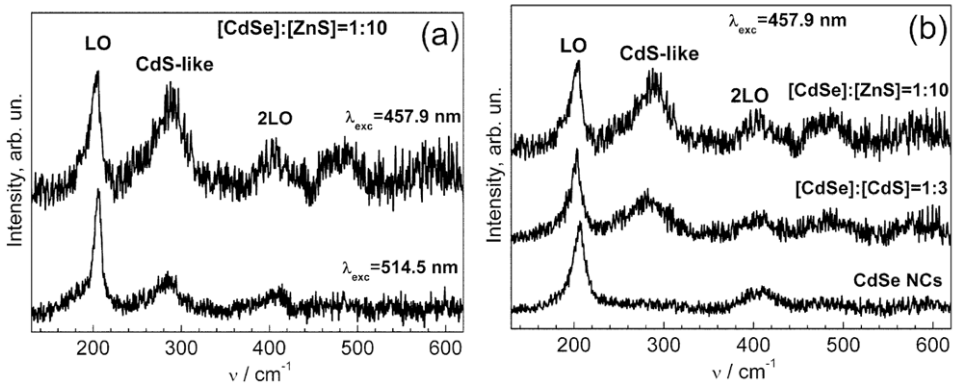

Figure 4. (a) RRS spectra of CdSe/ZnS NCs for excited $\lambda_{exc} = 514.5$ and 457.9 nm; (b) RRS spectra of bare CdSe, CdSe/CdS and CdSe/ZnS NCs for $\lambda_{exc} = 457.9$ nm.

shell thickness can preclude necessary resonance conditions even for $\lambda_{exc} = 441.7$ nm, though ZnS shell in [14] was detected with $\lambda_{exc} = 476.5$ nm. The formation of a mixed CdZnS(Se) alloy layer can lead to the appearance of a Raman peak at ∼290 cm^{-1} and also deteriorate the PL of this sample. Unfortunately, no Raman spectrum of satisfactory quality was obtained from the CdSe/ZnS sample with 'Zn—then S' passivation procedure because of the intense PL of the sample.

One could conclude from the Raman spectra of CdSe/ZnS NCs where the peak in the range of CdS LO phonon is detected while the band for the expected Zn–S vibrations is missing, that a ZnS shell is not formed at all and CdS is formed instead. However, we observed a similar picture for some commercially available CdSe/ZnS NCs, for which the formation of the shell was confirmed by independent techniques. Therefore, we conclude that the ZnS phonon does not contribute to the Raman spectrum because the electronic transition energies in the ZnS shell are too high and cannot be reached for resonance with available excitation wavelengths. The lowest electronic transition in a CdS shell for CdSe/CdS or a mixed interface layer for CdSe/ZnS NCs can obviously be reached with the wavelengths used here for excitation of the Raman spectra, even when the shell is as thin as a few MLs.

Further we discuss some observations in the Raman spectra of the passivated samples related to the resonant nature of the scattering. First, a strong dependence of the relative intensity of CdS- to CdSe-like peak on λ_{exc} was observed. The decrease of λ_{exc} from 528.7 nm down to 441.7 nm was accompanied with a continuous growth of the relative intensity of CdS-like peak. The spectra excited with 457.9 and 514.5 nm are presented in figure 3 to illustrate such dependence. This observation can be explained as follows. Excitation with the 514.5 nm line falls into the first absorption maximum of the NCs and, therefore, is most efficient in enhancement of the scattering by phonons localized inside the NCs. When λ_{exc} is decreased down to 457.9 nm, the excitation energy shifts away from the absorption maximum and, presumably, approaches the resonance with the electronic transition(s) related to the CdS shell. The existence of such an electronic transition was directly identified in [15]. An alternative explanation of the higher CdS peak intensity under excitation with a shorter wavelength can be the thicker shell in smaller NCs, which predominantly contribute to the RRS spectrum at higher excitation energy. The latter assumption can be partially confirmed by the slight high-frequency shift of the CdS peak accompanying its intensity increase (the thicker the passivation shell the weaker is the shell phonon confinement and the more efficiently can the shell withstand the tensile stress induced by the NC core). A similar behaviour was observed for CdTe/CdS NCs [16]. The frequency of the SO phonon, ν_{SO}, which is higher at $\lambda_{exc} = 457.9$ nm for bare CdSe NCs, increases even more, relative to $\lambda_{exc} = 514.5$ nm, in the passivated samples. This observation can also be the evidence of the larger shell-induced compressive strain in smaller NC cores which are probed with this shorter wavelength. However, the effect of the shell composition on ν_{SO} cannot be excluded as well [37]. The dependence of a shell-related LO peak intensity on λ_{exc} was also reported in [16] for CdTe/CdS NCs.

The stoichiometry of the shells is still questionable even for CdS passivation, because simultaneously with the peak at 300 cm^{-1} one more feature protrudes near 480–490 cm^{-1} in all the passivated samples (figures 2–4). It is known that, in the case of CdS_xSe_{1-x} alloys, the latter frequency is the sum of CdS- and CdSe-like phonons ($LO_{CdS} + LO_{CdSe}$) [31, 38, 44]. The observation of this spectral feature may be regarded as the evidence of a CdS_xSe_{1-x} (or even $Cd_{1-y}Zn_yS_xSe_{1-x}$ in the case of ZnS shell) alloy formation at the core–shell interface. The intensity of the combined modes for multimode systems was shown to be comparable or even higher than that of overtones [44]. Alloying can also explain a slight decrease of the CdSe LO phonon frequency after the passivation (see table 1) due to partial consumption of the core needed for the formation of the alloy. Note that, despite the moderate temperatures used in the current synthetic route (18–20 °C), the probability of alloying (interdiffusion) can be enhanced due to the lattice mismatch-induced non-homogeneous strain [39].

Formation of a ternary alloy at the core–shell interface was assumed in [11] for CdSe/ZnSe, based on an additional feature in Raman spectrum in the frequency region of the Zn(Cd)–Se phonon. The authors of [16] observed an additional Raman peak attributed to a CdS_xTe_{1-x} interlayer with $x \approx 0.35$ and reduction of the NC core diameter caused by the formation of the interlayer.

One more effect which can result in the downward shift of the CdSe LO phonon peak due to the NC passivation is directly related to the resonant and size-selective nature of the

Raman scattering and does not necessarily involve alloying. Formation of any shell shifts the absorption spectrum of the NCs towards the 'red' side by 3–17 nm (table 1). This means that resonant conditions for the same λ_{exc} in the passivated NCs will be fulfilled for NCs with smaller core size, as compared to the non-passivated ones. The smaller core size should induce stronger confinement on the phonons and, therefore, shift the CdSe peak to lower frequencies, as actually observed. Even if the compressive strain accompanies the shell growth (the higher frequencies of the surface mode in capped NCs can be the evidence of this), the downward shift is dominating for all the samples. However, if sampling smaller cores in the passivated NCs is assumed, one would expect broadening of the LO peak which is also the consequence of the phonon confinement. The absence of the expected broadening may be due to the narrowing of the 'resonant' region of the NC size for smaller NCs [40]. However, the latter fact needs a quantitative study.

The observed frequency of the CdS-like phonon is higher for CdSe/ZnS than for the CdSe/CdS sample with [CdSe]:[CdS] = 1:3 at approximately the same frequency of the CdSe (core) phonon. This is especially pronounced for $\lambda_{exc} = 457.9$ nm (figure 4). The observation can be explained by different shell thickness or/and composition. In particular, incorporation of Zn into the alloyed layer—i.e. formation of a $Cd_{1-y}Zn_yS_xSe_{1-x}$ alloy can increase the frequency of the $Cd_{1-y}Zn_yS$-like phonon [41].

An assignment of the peak at 480–490 cm^{-1} to a multiphonon Raman process without the assumption of alloying was also assumed, similar to the existence of a common resonance region for optical phonons in core and shell assumed in [16, 42].

Along with the downwards shift, following the shell deposition, the CdSe(core)-related peak undergoes a remarkable decrease in the width, which can result from a improved surface quality of CdSe NCs, in accordance with the PL results (table 1). The larger FWHM values for Raman peaks excited with 457.9 nm are obviously the result of the size-selective RRS process and are related to sampling of the smaller NCs which reveal larger confinement-induced broadening of the phonon peak.

4. Conclusions

CdSe nanocrystals possessing a near-bandgap photoluminescence were synthesized at relatively mild conditions from cadmium sulfate and sodium selenosulfate in aqueous solutions using gelatin as a stabilizer. Noticeable redshifts in absorption and PL spectra of the NCs after passivation with CdS and ZnS are accompanied with an improvement of their emission properties. Raman scattering spectra of the passivated NCs revealed new peaks attributed to the formation of passivating shells around CdSe cores. Significant changes in the spectra at different excitation wavelengths and shell formation parameters are related to the resonant and size-selective nature of Raman processes. The shifts in absorption and PL spectra, caused by passivation, are found to be in good agreement with relevant modification of the phonon spectra of NCs. The frequency of the CdS-like Raman peak, experimentally observed for the CdS-passivated NCs, is somewhat lower than the bulk CdS LO phonon frequency and correlates with that observed in [33] for thin CdS layers. For ZnS-passivated NCs a peak is observed at 280–290 cm^{-1}; however, no feature in the range of ZnS-related LO phonon is revealed. The reason for this can be a large bandgap of the ZnS shell, disabling the resonant conditions necessary for Raman signal to be achieved. Meanwhile, the appearance of the band in the CdS-like LO phonon range in the spectra of CdSe/ZnS NCs is explained by alloying at the core–shell interface or even formation of a completely mixed CdZnSSe shell.

Acknowledgments

VD is grateful to the Alexander von Humboldt Foundation for financial support during his research stay at Chemnitz University of Technology. The work was also partially supported by Fundamental Researches State Fund of Ukraine.

References

[1] Schmid G (ed) 2004 *Nanocrystals: From Theory to Application* (Weinheim: Wiley–VCH) and the references therein
[2] Peng X, Schlamp M C, Kadavanich A V and Alivisatos A P 1997 *J. Am. Chem. Soc.* **119** 7019
[3] Spanhel L, Haase M, Weller H and Henglein A 1987 *J. Am. Chem. Soc.* **109** 5649
[4] Khomutov G B and Koksharov Yu A 2006 *Adv. Colloid Interface Sci.* **122** 119
[5] Danek M, Jensen K F, Murray B C and Bawendi G M 1996 *Chem. Mater.* **8** 173
[6] Hines M A and Sionnest P G 1996 *J. Phys. Chem.* **100** 468
[7] Pradhan N, Katz B and Efrima S 2003 *J. Phys. Chem.* B **107** 13843
[8] Dabbousi B O, Rodriguez-Viejo J, Mikulec F V, Heine J R, Mattoussi H, Ober R, Jensen K F and Bawendi M G 1997 *J. Phys. Chem.* B **101** 9463
[9] Mekis I, Talapin D V, Kornowski A, Haase M and Weller H 2003 *J. Phys. Chem.* B **107** 7454
[10] Mokari T and Banin U 2003 *Chem. Mater.* **15** 3955
[11] Lee H, Holloway P H and Heesun Y 2006 *J. Chem. Phys.* **125** 164711
[12] Lee Y-J, Kim T-G and Sung Y-M 2006 *Nanotechnology* **17** 3539
[13] Xie R, Kolb U, Li J, Basche T and Mews A 2005 *J. Am. Chem. Soc.* **127** 7480
[14] Baranov A V, Rakovich Yu P, Donegan J F, Perova T S, Moore R A, Talapin D V, Rogach A L, Masumoto Y and Nabiev I 2003 *Phys. Rev.* B **68** 165306
[15] Singha A, Satpati B, Satyam P V and Roy A 2005 *J. Phys.: Condens. Matter* **17** 5697
[16] Schreder B, Schmidt T, Ptatschek V, Spanhel L, Materny A and Kiefer W 2000 *J. Cryst. Growth* **214/215** 782
[17] Raevskaya A E, Stroyuk A L and Kuchmiy S Ya 2006 *Colloid Interface Sci.* **302** 133–41
[18] Brus L 1986 *J. Phys. Chem.* **90** 2555
[19] Yu W W, Qu L, Guo W and Peng X 2003 *Chem. Mater.* **15** 2854
[20] Rogach A L, Kornowski A, Gao M, Eychmüller A and Weller H 1999 *J. Phys. Chem.* B **103** 3065
[21] Chestnoy N, Harris T D, Hull R and Brus L E 1986 *J. Phys. Chem.* **90** 3393
[22] Pesika N S, Stebe K J and Searson P C 2003 *J. Phys. Chem.* B **107** 10412
[23] Raevskaya A E, Stroyuk A L, Kuchmiy S Ya, Dzhagan V M, Valakh M Ya and Zahn D R T 2007 *J. Phys.: Condens. Matter* submitted

[24] Plotnichenko V G, Mityagin Yu A and Vodop'yanov L K 1977 *Sov. Phys.—Solid State* **19** 1584
[25] Hwang Y N, Shin S, Park H L, Park S H and Kim U 1996 *Phys. Rev.* B **54** 15120
[26] Tanaka A, Onari S and Arai T 1992 *Phys. Rev.* B **45** 6587
[27] Campbell I H and Fauchet P M 1986 *Solid State Commun.* **58** 739
[28] Faraci G, Gibilisco S, Russo P, Pennisi A R and La Rosa S 2006 *Phys. Rev.* B **73** 033307
[29] Meulenberg R W, Jennings T and Strouse G F 2004 *Phys. Rev.* B **70** 235311
[30] Rodden W S O, Torres C M S and Ironside C N 1995 *Solid State Commun.* **10** 807
[31] Roy A and Sood A K 1996 *Phys. Rev.* B **53** 12127
[32] Leite R C C and Porto S P S 1966 *Phys. Rev. Lett.* **17** 10
[33] Zou S and Weaver M J 1999 *J. Phys. Chem.* B **103** 2323
[34] Comas F, Trallero-Ginner C, Studart N and Marques G E 2002 *Phys. Rev.* B **65** 073303
[35] Zhang J-Yu, Wang X-Y, Xiao M, Qu L and Peng X 2002 *Appl. Phys. Lett.* **81** 2076
[36] Dinger A, Hetterich M, Goppert M, Grun M, Klingshirn C, Weise B, Liang J, Wagner V and Geurts J 1999 *J. Cryst. Growth* **200** 391
[37] Mlayah A, Brugman A M, Carles R, Renucci J B, Valakh M Ya and Pogorelov A V 1994 *Solid State Commun.* **90** 567
[38] Azhniuk Yu M, Milekhin A G, Gomonnai A V, Lopushansky V V, Yukhymchuk V O, Schulze S, Zenkevich E I and Zahn D R T 2004 *J. Phys.: Condens. Matter* **16** 9069
[39] Krasil'nik Z K, Lytvyn P, Lobanov D N, Mestres N, Novikov A V, Pascual J, Valakh M Ya and Yukhymchuk V A 2002 *Nanotechnology* **13** 81
[40] Trallero-Giner C, Debernardi A, Cardona M, Menendez-Proupın E and Ekimov A I 1997 *Phys. Rev.* B **57** 4664
[41] Azhniuk Yu M, Milekhin A G, Gomonnai A V, Lopushansky V V, Turok I I, Yukhymchuk V O and Zahn D R T 2004 *Phys. Status Solidi* a **201** 1578
[42] Manciu F S, Tallman R E, McCombe B D, Weinstein B A, Lucey D W, Sahoo Y and Prasad P N 2005 *Physica* E **26** 14
[43] Kulish N R, Kunets V P and Lisitsa M P 1997 *Superlatt. Microstruct.* **22** 341
[44] Valakh M Ya, Klochikhin A A and Litvinchuk A P 1984 *Sov. Phys.—Solid State* **26** 113